Journal of Pharmaceutical and Biomedical Analysis 204 (2021) 114247

Contents lists available at ScienceDirect

Journal of Pharmaceutical and Biomedical Analysis

journal homepage: www.elsevier.com/locate/jpba

Metabolic profile of irradiated whole blood by chemical isotope-labeling liquid chromatography-mass spectrometry

Xuan Lu[a,1], Xinli Zhu[b,1], Deying Chen[a], Jiahang Zhou[a], Jiong Yu[a], Jue Xie[c,e], Senxiang Yan[b,**], Hongcui Cao[a,e,*], Liang Li[d], Lanjuan Li[a]

[a] State Key Laboratory for Diagnosis and Treatment of Infectious Diseases, National Clinical Research Center for Infectious Diseases, The First Affiliated Hospital, Zhejiang University School of Medicine, 79 Qingchun Rd, Hangzhou City, Zhejiang Province, 310003, China
[b] Department of Radiation Oncology, The First Affiliated Hospital, Zhejiang University School of Medicine, 79 Qingchun Rd., Hangzhou City 310003, China
[c] Department of Blood Transfusion, The First Affiliated Hospital, Zhejiang University School of Medicine, 79 Qingchun Rd., Hangzhou City 310003, China
[d] Department of Chemistry, University of Alberta, Edmonton, Alberta T6G 2G2, Canada
[e] Zhejiang Provincial Key Laboratory for Diagnosis and Treatment of Aging and Physic-chemical Injury Diseases, 79 Qingchun Rd, Hangzhou City 310003, China

ARTICLE INFO

Article history:
Received 12 January 2021
Received in revised form 28 June 2021
Accepted 3 July 2021
Available online 6 July 2021

Keywords:
Irradiated blood
Metabolomics
Chemical isotope labeling
Liquid chromatography-mass spectrometry

ABSTRACT

Irradiated blood is a new type of blood product used to prevent transfusion-associated graft-versus-host disease. However, the effects of irradiation on the metabolism of plasma, red blood cells (RBCs), and peripheral blood mononuclear cells (PBMCs) are largely unknown. We developed a workflow for testing metabolic changes in whole blood to determine the impact of irradiation by chemical isotope labeling liquid chromatography-mass spectrometry (CIL LC–MS). Blood parameters, PBMC proliferation and apoptosis were examined before and after irradiation. Next, the amine/phenol metabolites in the blood components were assayed by ^{12}C- and^{13}C-dansylation labeling LC–MS. We identified 1654, 1730, and 1666 peak pairs in plasma, RBCs, and PBMCs, respectively. We screened out 367, 177, and 219 significant metabolites in plasma, RBCs, and PBMCs, respectively, by principle component analyses, volcano plots, and Venn plots. Metabolic pathway analyses showed that irradiation modulated taurine and hypotaurine metabolism in plasma and purine metabolism in RBCs and PBMCs. Changes in potential biomarkers, including an increase in hypoxanthine level and a decrease in adenine level, may be related to the dysfunction of DNA synthesis in PBMCs. The decreased AMP level in RBCs may interfere with RBC storage lesions. Our research provides a more comprehensive perspective on blood metabolism associated with irradiation.

1. Introduction

Blood and blood component transfusions are common practices in clinical care. Irradiated blood is a new type of blood product, consisting of irradiated whole blood or its components [1]. Gamma or X-irradiation at a dose of 25–50 Gy is recommended [2].

Irradiated blood is mainly used to prevent transfusion-associated graft-versus-host disease (TA-GVHD). TA-GVHD is an uncommon but fatal transfusion complication with a survival rate < 10 %, which affects the skin, bone marrow, liver, and gastrointestinal tract within 1–2 weeks of transfusion [3,4]. TA-GVHD occurs in immunocompromised patients, immunocompetent individuals, and in the presence of non-histocompatibility between recipient and donor [5]. Under these conditions, cytotoxic CD8$^+$ T lymphocytes are activated by foreign human leukocyte antigens, resulting in the activation of helper CD4$^+$ T lymphocytes, inducing lymphocytes to engraft, proliferate, and attack the host [6]. Lymphocytes

Abbreviations: TA-GVHD, transfusion-associated graft-versus-host disease; PBMC, peripheral blood mononuclear cell; RBC, red blood cell; CIL LC–MS, chemical isotope labeling liquid chromatography-mass spectrometry; Dns, dansylation; PHA, phytohemagglutinin; MPA, mobile phase A; MPB, mobile phase B; FA, formic acid; ACN, acetonitrile; PCA, principal component analysis; FC, fold change; HMDB, human metabolome database; OD, optical density; PI, propidium iodide; QC, quality control; PRPP, phosphoribosyl pyrophosphate; IMP, inosine monophosphate; AMP, adenosine monophosphate; dGDP, deoxyguanosine diphosphate; GMP, guanosine monophosphate; GDP, guanosine diphosphate; ATP, adenosine-triphosphate.

* Corresponding author at: State Key Laboratory for the Diagnosis and Treatment of Infectious Diseases, The First Affiliated Hospital, Zhejiang University School of Medicine, 79 Qingchun Rd., Hangzhou City 310003, China.
** Corresponding author at: Department of Radiation Oncology, The First Affiliated Hospital, Zhejiang University School of Medicine, 79 Qingchun Rd., Hangzhou City 310003, China.
E-mail addresses: yansenxiang@zju.edu.cn (S. Yan), hccao@zju.edu.cn (H. Cao).
[1] These authors contributed equally to this work.

https://doi.org/10.1016/j.jpba.2021.114247

account for around 70 %–90 % of human peripheral blood mononuclear cells (PBMCs) [7]. Irradiation of blood can damage nuclear DNA of lymphocytes or indirectly inhibit their proliferation [8].

Based on previous reports and the guidelines of the American Association of Blood Banks, blood should be irradiated within 14 days of collection and the storage period of irradiated blood should not exceed 14 days [9,10]. At present, irradiated blood products commonly used in clinical practice include whole blood, suspended red blood cells, and apheresis platelets. Red blood cells (RBCs), plasma, and PBMCs are present in blood products, such as whole blood and suspended RBCs, and their metabolism may be influenced by irradiation. In the field of transfusion medicine, metabolomics studies have mainly concentrated on descriptive correlative associations and testing simple aspects, such as the metabolism of potassium and ATP [11]. However, few metabolic studies have systematically and quantitatively discussed the effects of irradiation on the metabolism of RBCs, PBMCs, and plasma.

Metabolomics is a comprehensive and systematic study of small molecule (< 1000 Da) metabolites in biological samples or organs [12,13]. Liquid chromatography-mass spectrometry (LC–MS) is a commonly used method in metabolomics because of its high sensitivity and specificity [14,15]. The purpose of metabolomics is to study changes in the dynamic state of metabolites in the process of metabolism. To increase the detection rate, quantitative accuracy, and coverage of metabolites, high-performance chemical isotope labeling (CIL) LC–MS has been used [16,17]. This technique involves the labeling of metabolites in two samples to be compared using differential isotope markers, followed by LC–MS analysis [18]. With appropriate design of labeling reagents, CIL LC–MS can substantially improve the detectability of a class of metabolites, and improve the separation efficiency of LC and the sensitivity of MS [19]. For example, metabolites containing amines/phenols can be profiled by LC–MS with labeling by $^{12}C/^{13}C$-dansylation (Dns) [20]. Compared with traditional LC–MS, CIL LC–MS can generate more accurate and stable relative quantitative results [21,22].

We assayed the proliferation and apoptosis of irradiated and non-irradiated PBMCs by CCK-8 viability assay after phytohemagglutinin (PHA) stimulation and by flow cytometry. We also quantified metabolites in plasma, RBCs, and PBMCs from irradiated and non-irradiated whole blood by $^{12}C/^{13}C$-Dns labeling LC–MS. We assessed the levels of metabolites and changes in metabolic pathways, as well as the underlying mechanisms. The use of $^{12}C/^{13}C$-Dns labeling LC–MS enabled quantification and further understanding of the effects of irradiation on blood cells and plasma metabolites.

2. Material and methods

2.1. Study design

We obtained whole blood from 22 donors (22–35 years old) consisting of 10 males and 12 females. All donors met the whole blood and component donor selection requirements of the People's Republic of China.

Each donation of whole blood underwent routine blood tests and was split into two bags on the day of collection (day 0). One of each pair of bags was irradiated on the first day after collection (day 1) at a dose of 25 Gy using a Gamma-Ray Irradiator (CIF Medical, HK II, Beijing, China); the control group comprised all non-irradiated second bags of the pairs. We performed routine blood tests on all samples after irradiation. Each bag of blood was tested for serum potassium and RBC adenosine triphosphate (ATP) content to confirm the quality of samples before and after irradiation. Potassium was assayed using an automated analyzer (Olympus AU 640; Olympus Europe, Hamburg, Germany). ATP was detected by CellTiter-Glo® Luminescent Cell Viability Assay (Promega, Madison, WI, USA) and the luminescence was determined using a luminometer (GloMax96; Promega). We isolated RBCs, plasma, and PBMCs from whole blood and extracted metabolites. PBMC proliferation and apoptosis were evaluated by CCK-8 assays and flow cytometry, respectively. The study was approved by the Ethics Committee of The First Affiliated Hospital, Zhejiang University School of Medicine, Zhejiang, China.

2.2. Isolation of plasma and metabolite extraction

Samples were centrifuged for 10 min at 800 × g (Microfuge 22R centrifuge; Beckman Coulter; Brea, CA, USA) to stratify blood. Plasma (90 μL) was aspirated from the top layer of each sample and a threefold volume of methanol precooled to −20 °C was added (Fisher Chemical, Waltham, MA, USA). Insoluble proteins were pelleted by centrifugation (30 min at 4 °C and 15,000 rpm) and supernatants were collected and dried in a refrigerated CentriVap concentrator system (Labconco, Kansas City, MO, USA).

2.3. Isolation of RBCs and metabolite extraction

RBCs (500 μL) were extracted from the specimens, washed twice in 2 mL of phosphate-buffered saline (PBS) (Servicebio, Wuhan, China), and centrifuged for 10 min at 2500 × *g*; the supernatant was discarded. Next, 60 μL of RBCs was extracted with 540 μL of lysis buffer (methanol:acetonitrile:water, 5:3:2, v/v; Fisher Chemical) [23]. The mixture was vortex-mixed at 2500 rpm for 1 min and transferred to an ice bath for 1 min; this mixing and ice bath incubation protocol was performed five times. The samples were centrifuged for 30 min at 15,000 × *g* at 4 °C and the supernatants were collected and dried down as described above.

2.4. Isolation of PBMCs and metabolite extraction

Blood was diluted 1:1 with PBS before placement on a layer of Ficoll (GE Healthcare, Stockholm, Sweden), and centrifuged at 2000 rpm for 20 min. White flocculent PBMC layers were separated. Next, 1 mL of methanol:water mixture (1:1, v/v, −20 °C, Fisher Chemical) was added to the PBMCs, which were transferred to 1.5 mL centrifuge tubes (Thermo Scientific) and centrifuged for 4 min at 1200 rpm at 4 °C. A 900-μL aliquot of the supernatant was removed and stored for later use. Next, 0.5 mL of glass beads (Biospec Products Inc., Bartlesville, OK, USA) 1.0 mm in diameter were added to the pellet, which was oscillated at 2500 rpm on a Touch Mixer Model 232 (Fisher Scientific, USA) for 1 min and transferred to an ice bath for a further 1 min, this mixing and ice bath incubation protocol was performed 10 times. Next, 900 μL of supernatant was added, followed by centrifugation for 30 min at 16,000 × *g* [24]. Finally, the supernatants were collected and dried down as described above.

2.5. Dansylation labeling and LC–MS

Dried metabolites were dissolved in ultrapure water (Sigma-Aldrich, St. Louis, MO, USA) for $^{12}C/^{13}C$-Dns labeling. We used light-chain ^{12}C-dansyl chloride (Sigma-Aldrich, St. Louis, MO, USA) to label individual samples and heavy-chain ^{13}C-dansyl chloride to label pooled samples. The pooled samples were generated by mixing individual samples at equimolar concentrations.

Metabolites (25 μL) were mixed with 12.5 μL of sodium carbonate/sodium bicarbonate buffer (0.5 M, pH 9.5; Sigma-Aldrich) and 12.5 μL of acetonitrile (Sigma-Aldrich). Next, 25 μL of ^{12}C-dansyl chloride or ^{13}C-dansyl chloride (20 mg/mL; Sigma-Aldrich) was added and the mixture was vortex-mixed for 10–15 s. The reaction mixture was placed in a 40 °C water bath for 1 h. NaOH (5 μL,

250 mM; Sigma-Aldrich) was added, incubated for 10 min, and the reaction was neutralized by adding 25 μL of formic acid.

The $^{12}C/^{13}C$-Dns mixture was centrifuged at 15,294 × *g* for 10 min and subjected to LC–MS. The labeled sample was analyzed using an UltiMate 3000 UHPLC system (Thermo Scientific) combined with an Impact II quadrupole time-of-flight (QTOF) mass spectrometer (Bruker, Billerica, MA, USA). A reverse-phase column (ACQUITY UPLC BEH C_{18} column, 2.1 mm ×15 cm, 1.7 μm particle size; Waters Corporation, Milford, MA, USA) was used to separate the Dns-labeled metabolites. Mobile phase A (MPA) was 0.1 % (v/v) formic acid (FA) in water, and mobile phase B (MPB) was 0.1 % (v/v) FA in acetonitrile (ACN). The gradient profile for metabolite separation was: t =0 min, 25 % B; t =10 min, 99 % B; t =13 min, 99 % B; t =13.1 min, 25 % B; and t =16 min, 25 % B. The flow rate was 0.4 mL/min, and the column temperature was maintained at 40 °C. All mass spectra were collected in positive ion mode at an acquisition rate of 1 Hz. The individual samples were arranged in a random sequence during LC–MS analysis. The quality control (QC) mixture was prepared by mixing the ^{12}C- and ^{13}C-labeled pooled samples at an equivalent total metabolite amount. Throughout data acquisition, a QC run was conducted after every 20 samples to monitor instrument performance.

2.6. PBMC proliferation assay

Isolated PBMCs were stimulated with PHA (Absin Bioscience, Inc., Shanghai, China) for 3 days at 37 °C in a 5% CO_2 incubator (HERA-Cell® 150; Thermo Fisher Scientific). PHA at 5 μg/mL was added to a 96-well plate (1–2 × 10^5 cells/well) containing 1640 Roswell Park Memorial Institute (RPMI) medium (Life Technologies Corporation, NY, USA) and 10 % fetal bovine serum (FBS); the blank group didn't add cells. The cells were observed under an electron microscope (Eclipse TS100; Nikon, Tokyo, Japan). After 3 days, CCK-8 reagent (BD Biosciences, Franklin Lakes, NJ, USA) at 10 μL/well was added to the 96-well plate, followed by incubation for 4 h. The absorbance at 450 nm was determined using a microplate reader. The experiment was performed in triplicate [25].

$$\text{Inhibition of proliferation (\%)} = 1 - \frac{[\text{OD (irradiated group)} - \text{OD (blank group)}]}{[\text{OD (control group)} - \text{OD (blank group)}]} \times 100\%$$

2.7. PBMC apoptosis assay

An Annexin V 633 Apoptosis Detection Kit (BD Biosciences) was used to assess apoptosis of PBMCs. PBMCs were resuspended in 1× Annexin V binding solution to 1 × 10^6/mL. Next, Annexin V-633 binding compound (5 μL) was added to 100 mL of cell suspension, followed by 5 μL of propidium iodide (PI). After incubation at room temperature in the dark for 15 min, 400 μL of Annexin V binding solution was added and the samples were subjected to flow cytometry (BeamCyte-1026; Beamdiag, Changzhou, China) within 1 h.

2.8. Data analyses

IsoMS software is used for analyzing large amounts of raw data generated by LC–MS through peak pair intensity ratio; it creates a file that includes retention times and accurate mass information [26]. Metabolites without detectable peaks can be filled in using zero-fill software [27]. IsoMS-Quant was used to determine the chromatography peak-intensity ratio [18].

Our approach of using accurate mass and retention time searches against the dansyl standard library for metabolite identification was described previously [28]. Briefly, the retention time of LC–MS runs was corrected or normalized using a set of 25 dansyl-labeled standards with a retention time (RT) of approximately 1–2 min covering the entire RT window of the LC separation. The same set of standards was used for normalizing a dansyl-labeled standard metabolite during the construction of the dansyl library. Using this approach, the normalized RT of an unknown metabolite can be directly compared with library standards to identify a possible match. In addition, we compared the RT with the predicted retention time of each dansyl-labeled compound in the HMDB compound library. Among the list of mass-matched metabolites, their retention times were different and therefore we could find a unique identification based on mass and RT.

Unsupervised principal component analysis (PCA) was performed using SIMCA-P^+ 12.0 software (Umetrics, Umeå, Sweden) to examine the data quality (e.g., to identify outliers). Then univariate analysis (i.e., volcano plot) was used to analyze the differential metabolites.

Differential metabolites were selected based on the paired *t*-test and fold change (FC) determined by SPSS (ver. 21.0; IBM Corp., Armonk, NY, USA). Statistical significance was accepted at $p < 0.05$ and FC ≥ 1.2. Differential metabolic pathways were analyzed by metaboAnalyst ver. 3.0. Flow cytometry data were analyzed using Flow Jo software (ver. 10.6.2; Tree Star, Inc., Ashland, OR, USA).

3. Results

3.1. Changes in blood parameters after irradiation

The routine blood parameters of the donors are shown in Supplementary Table S1. We classified leukocytes as neutrophils, lymphocytes, monocytes, eosinophils, and basophils. In females, the proportion of monocytes increased and the number of lymphocytes decreased; in males, the decreases in count and proportion of granulocytes were accompanied by increases in the number of white blood cells and the proportions of lymphocytes and monocytes. Moreover, the hematocrit and mean corpuscular volume were increased in males. The serum potassium level and RBC ATP level did not change significantly before and after blood irradiation, suggesting that irradiation did not significantly alter the quality of blood (Supplementary Fig. S1).

3.2. Effects of irradiation on the proliferation and apoptosis of PBMCs

PHA stimulation triggers the transformation of dormant lymphocytes into lymphoblasts, resulting in increased DNA synthesis, cell size, and cytoplasm (Fig. 1A). Lymphocyte enrichment was obvious in the control group, but was reduced in the irradiated group. CCK-8 can be combined with succinic dehydrogenase in the mitochondria of cells with proliferation activity to form water-soluble formazans, which show maximum absorbance at a wavelength of 450 nm. The proliferation viability of PBMCs in the irradiated group was 49.28 %, compared with the control group (Fig. 1B). The PBMCs in the irradiated group showed 50.72 % inhibition of proliferation, compared with the control group.

The apoptosis rates of PBMCs are shown in Fig. 1C. The Q3 quadrant shows early apoptotic cells (Annexin V^+ and PI^-), and the Q2 quadrant shows late apoptotic cells (Annexin V^+ and PI^+). In addition, the rates of damage in the control and irradiated groups caused by experimental treatments in the Q2 quadrant were 1.1 % and 2.1 %, respectively, indicating good quality of collected PBMCs. The apoptosis rates of PBMCs were 13.31 % and 7.57 % in the irradiated and control groups, respectively (Fig. 1D).

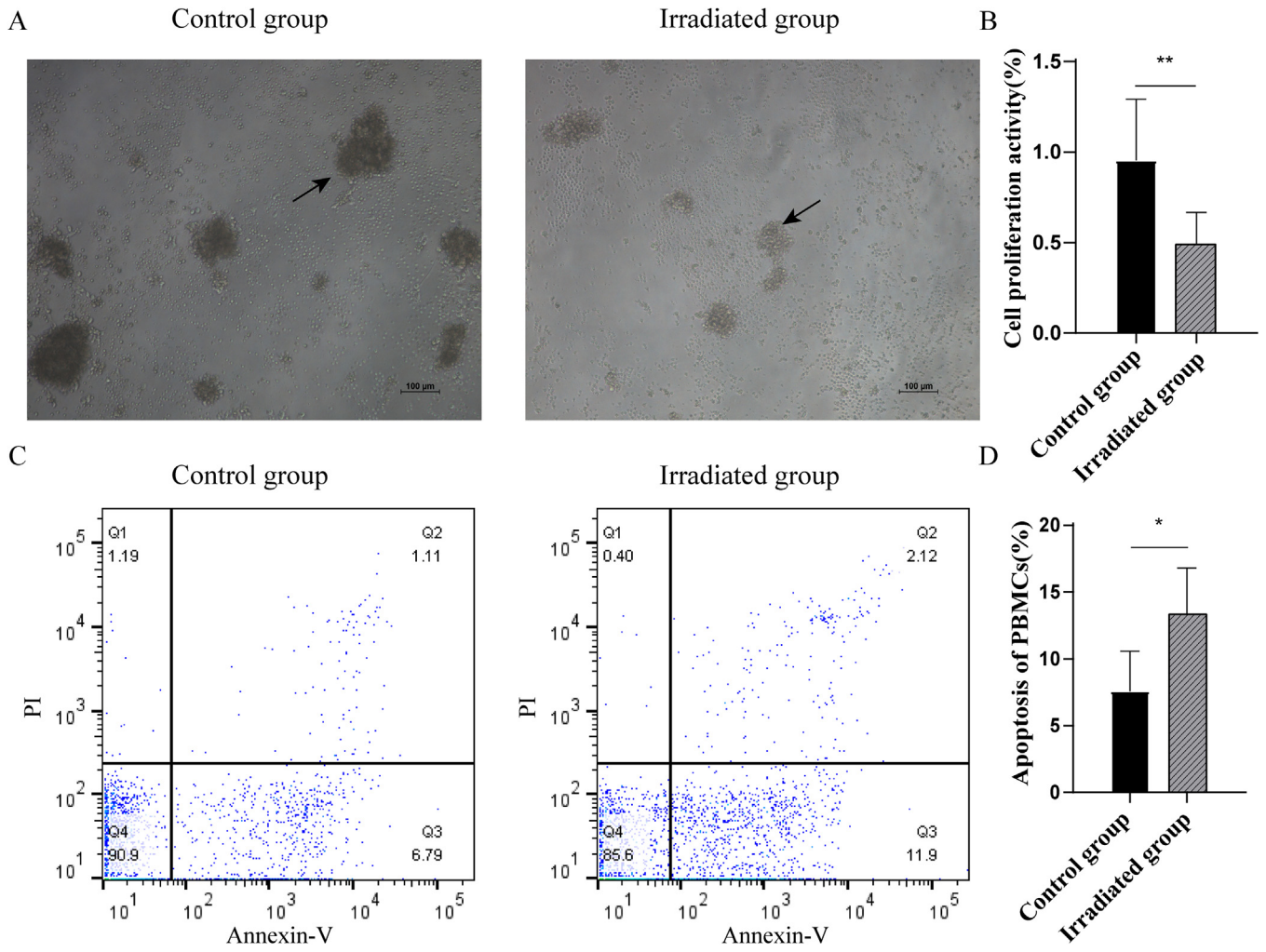

Fig. 1. Proliferation and apoptosis of PBMCs. **(A)** Lymphocytes transformed into lymphoblasts, characterized by increased DNA synthesis, cell volume, and cytoplasm after stimulation with PHA (arrow). **(B)** PBMC proliferation activity in the control and irradiated groups. **(C)** Apoptosis and necrosis were assayed using Annexin V/PI fluorescence. **(D)** PBMC apoptosis in the control and irradiated groups. Data are means ± SDs; $^{*}p < 0.05$, $^{**}p < 0.01$.

3.3. Metabolomics analysis of irradiated blood

Amine- and phenol-containing metabolites play major roles in metabolic pathways. The workflow shown in Fig. 2 indicates the process of CIL LC–MS analysis. Sample size was standardized for the mixtures of ^{12}C-labeled single samples and ^{13}C-labeled mixed samples; 2437, 2508, and 2493 peak pairs were detected in plasma, RBCs, and PBMCs, respectively.

3.3.1. Metabolomics analysis of plasma

Of the 1654 peak pairs detected, 303 were in the Dns standard library and 1351 were in the HMDB library (Supplementary Table S2). The agglomeration of QC samples in PCA plot indicated that the LC–MS method had good stability and repeatability (Fig. 3A). And Fig. 3A shows that there was an outlier in the control group. After taking this outlier out, we used the univariate analysis (i.e., volcano plot) to select the significantly changed metabolites. To screen for differential metabolites, paired *t*-test and FC values were used to compare changes in peak pairs. We chose peak pair intensity, which satisfied the requirement for $p < 0.05$ and FC ≥ 1.2. Volcano plots were used to filter differential peak pairs as indicated by red color in the graph. The levels of 367 peak pairs differed markedly, regardless of sex (Fig. 3B). We also used the volcano plots to determine the significantly changed metabolites between the females and males. 233 and 279 peak pairs showed significant changes in females and males, respectively (Supplementary Fig. S2A, B). Detailed results of peak pair comparisons are presented in a Venn diagram in Supplementary Fig. S2C.

12 significant metabolites were identified using the Dns standard library (Supplementary Table S3). MetaboAnalyst ver. 3.0 was used to conduct metabolic pathway analyses of these 12 metabolites. Supplementary Fig. S2D presents an overview of pathway analysis according to the pathway impact value and *p*-values. Taurine and hypotaurine metabolism was the pathway most significantly affected by irradiation in plasma, and hypotaurine was a potential biomarker of metabolism (Fig. 3C); the details of metabolites that were significantly changed are listed in Supplementary Table S4. The metabolic pathways in plasma are listed in Supplementary Table S5.

3.3.2. Metabolomics analysis of RBCs

A total of 275 peak pairs were detected in the Dns standard library and 1455 in the HMDB library, such that the total number was 1730 for RBCs (Supplementary Table S6). In the PCA score plot, QC samples clustered together and there was no obvious outlier in the analysis of metabolites for RBCs (Fig. 4A).

Significant peak pairs in RBCs are shown as a volcano plot (FC ≥ 1.2, $p < 0.05$) in Fig. 4B. Results of peak pair comparisons are

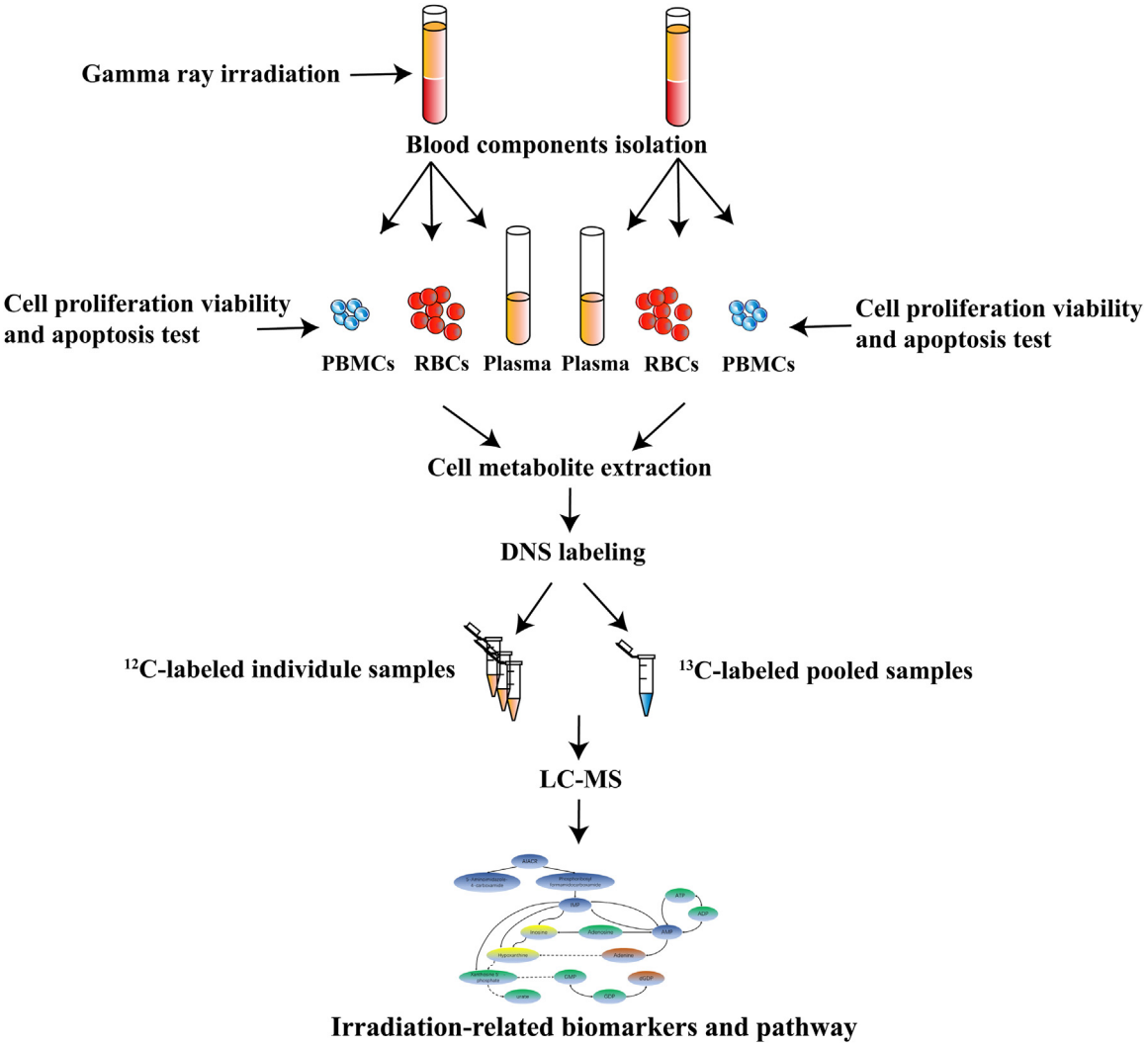

Fig. 2. Schematic of the overall workflow.

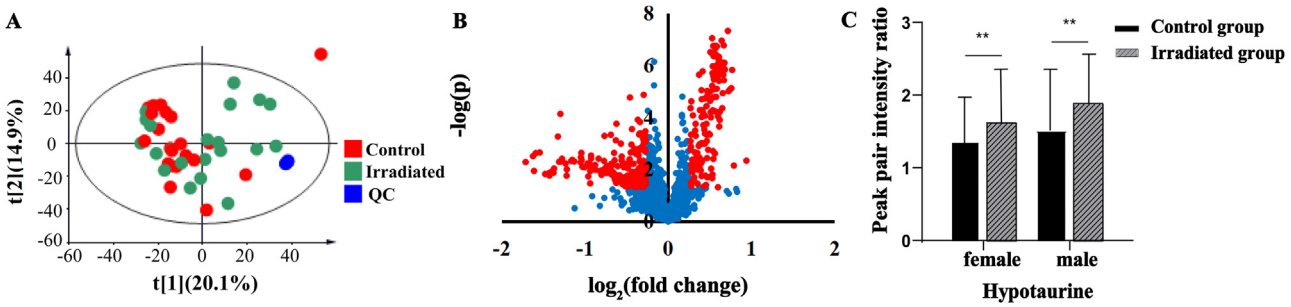

Fig. 3. Metabolome profiling of plasma. **(A)** PCA score plot for plasma peak pairs in the control and irradiated groups. **(B)** Volcano plots of irradiation-induced changes. Red, significant peak pairs (FC ≥ 1.2, $p < 0.05$). **(C)** Peak pair intensity ratios of significant metabolites in males and females. Data are means ± SDs; $^{**}p < 0.01$. (For interpretation of the references to colour in this figure legend, the reader is referred to the web version of this article).

presented in a Venn diagram in Fig. 4C. The levels of 177 peak pairs changed regardless of sex, and the levels of 134 and 176 changed in females and males (Supplementary Fig. S3A, B), respectively.

3.3.3. *Metabolomics analysis of PBMCs*

For PBMCs, 324 peak pairs were detected in the Dns standard library and 1342 pairs were inferred in the HMDB library (Supplementary Table S7). In the PCA score plot, the tight clustering of QC samples indicated high credibility and we found no obvious outlier to exclude in the analysis of metabolites for PBMCs (Fig. 4D).

The details of Venn diagram are shown in Supplementary Table S8. The levels of 219 peak pairs were altered by irradiation (Fig. 4E). The levels of 156 and 323 peak pairs changed markedly in females and males, respectively (Supplementary Fig. S3C, D). Significant peak pairs are shown in a Venn diagram in Fig. 4F.

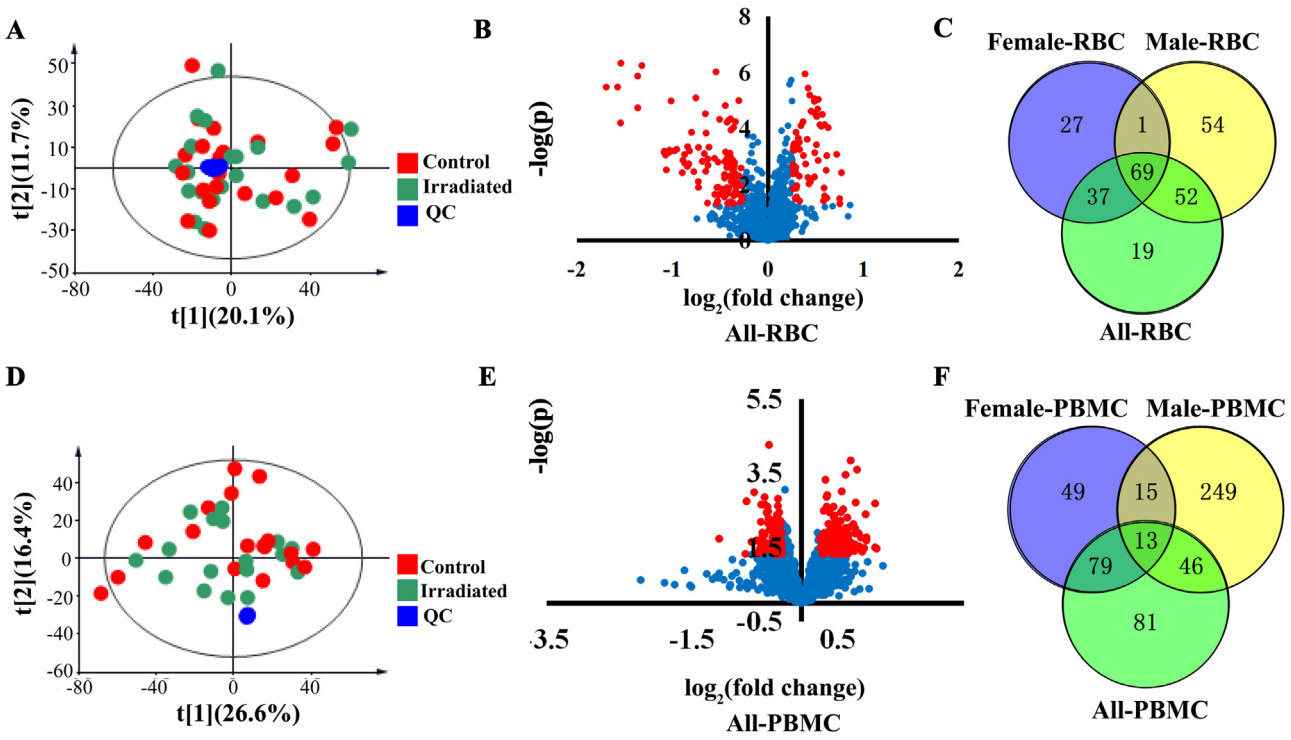

Fig. 4. Metabolome profiling of RBCs and PBMCs. **(A)** PCA score plot for RBC peak pairs in the control and irradiated groups. **(B)** Volcano plots of RBC irradiation-induced changes. Red, significant peak pairs (FC ≥ 1.2, $p < 0.05$). **(C)** Venn diagram of significant peak pairs in females, males, and all RBC samples. **(D)** PCA score plot for PBMC peak pairs. **(E)** Volcano plots of PBMC irradiation-induced changes. Red, significant peak pairs (FC ≥ 1.2, $p < 0.05$). **(F)** Venn diagram of significant peak pairs in females, males, and all PBMC samples. (For interpretation of the references to colour in this figure legend, the reader is referred to the web version of this article).

3.3.4. Biomarker selection and pathway analyses of RBCs and PBMCs

16 metabolites with differences in RBCs were detected in the standard library, and 39 metabolites were inferred by the zero-reaction library of HMDB (Supplementary Tables S9, 10). Among the differential metabolites in PBMCs, 21 were present in the standard library and 23 were identified in the zero-reaction library of HMDB (Supplementary Tables S11, 12). These metabolites were analyzed using MetaboAnalyst ver.3.0 to identify differential metabolic pathways in RBCs and PBMCs (Fig. 5A, B). Significant metabolic pathways of RBCs included aminoacyl-tRNA biosynthesis and purine metabolism. In contrast, the differential metabolic pathways in PBMCs were related to tryptophan and purine metabolism. Irradiation altered 11 and 20 metabolic pathways in RBCs and PBMCs, respectively (Supplementary Table S5). We identified the significant metabolites involved in the final pathway, then evaluated them according to sex (Fig. 5C, D). Fig. 6 presents a schematic illustration of the final pathway analysis results of changes in purine metabolism that occurred in both RBCs and PBMCs. 5-Aminoimidazole-4-carboxamide-1-β-D-ribofuranoside (AICAR), 5-aminoimidazole-4-carboxamide, phosphoribosyl formamidocarboxamide, inosine monophosphate (IMP), adenosine monophosphate (AMP), hypoxanthine, and inosine were decreased in RBCs. Adenine and deoxyguanosine diphosphate (dGDP) were decreased in PBMCs, while inosine and hypoxanthine were increased. The details of significant metabolites are listed in Table 1. The alterations of these metabolites seemed to be related to irradiation, and they may include potential biomarkers.

4. Discussion

In this study, we evaluated the effects of irradiation on plasma, RBC, and PBMC metabolism. The quality of blood after irradiation was confirmed by routine blood test and measurement of serum potassium and RBC ATP levels. Proliferation activity and apoptosis of PBMCs were examined by CCK-8 viability assay and flow cytometry. The results showed that 1654 of 2437 peak pairs (67.87 %) in plasma, 1730 of 2508 (68.98 %) in RBCs, and 1666 of 2493 (66.83 %) in PBMCs were present in the Dns standard library and HMDB. The detection of amine/phenol-containing metabolites after irradiation implied that $^{12}C/^{13}C$-dansylation labeling LC–MS provides comprehensive coverage. Unsupervised PCA score plot is sensitive to outliers and noise [29]. Therefore, PCA plot was used in this study to verify the stability of $^{12}C/^{13}C$-dansylation labeling LC–MS method and find outliers. We found an outlier in the analysis of plasma, so this set of data has been excluded in the subsequent search for differential metabolites in plasma. The final results suggested that irradiation altered metabolism in plasma, RBCs, and PBMCs. The differential metabolites were compared between gender, and the outcome indicated that the variation trend was almost the same between males and females. We next investigated the metabolic pathways related to metabolites that showed differences in levels; the results suggested that purine metabolism was altered in RBCs and PBMCs, while taurine and hypotaurine metabolism was altered in plasma.

CCK-8 test without PHA stimulation was performed to determine the viability of PBMCs in both control and irradiated groups. The results showed that there were no significant differences in PBMC viability before and after irradiation (data not shown). However, after stimulation of PBMCs with PHA, an exogenous agglutinin that promotes proliferation by binding to mitogen receptors on the lymphocyte cell membrane [25], we found that PBMC proliferation was significantly decreased by irradiation. Moreover, Annexin V-PI staining showed that irradiation promoted apoptosis of PBMCs. The observations indicated that irradiation does not immediately alter the viability of PBMCs, but changes their proliferation and apoptosis characteristics. These effects may be related to radiation-induced

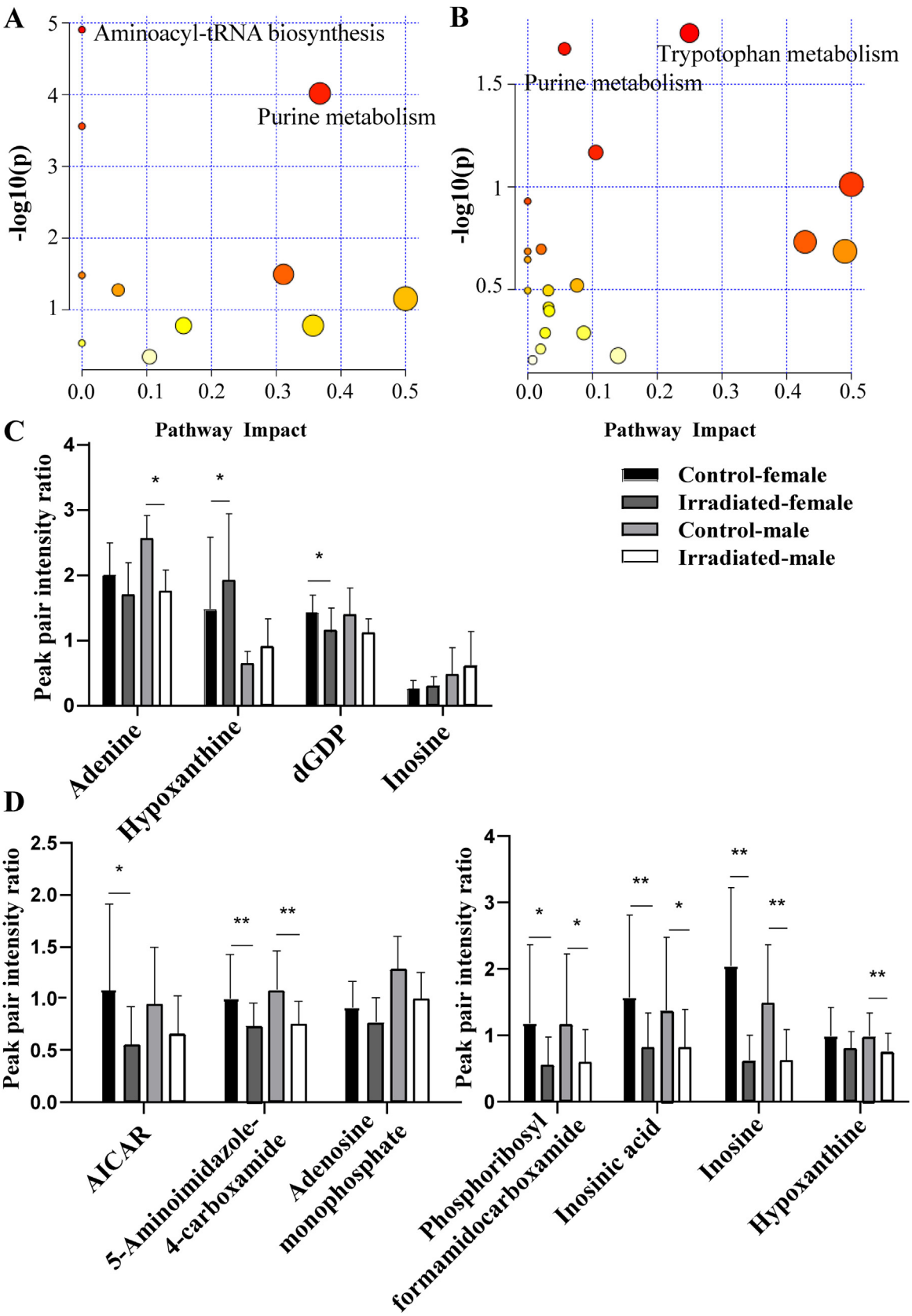

Fig. 5. Metabolic pathway and irradiation-related biomarker analyses of RBCs and PBMCs. Overview of pathway analyses for significant metabolites in **(A)** RBCs and **(B)** PBMCs. Peak pair intensity ratios of the control and irradiated groups, and according to sex in **(C)** PBMCs and **(D)** RBCs. Data are means ± SDs; $^{*}p < 0.05$, $^{**}p < 0.01$.

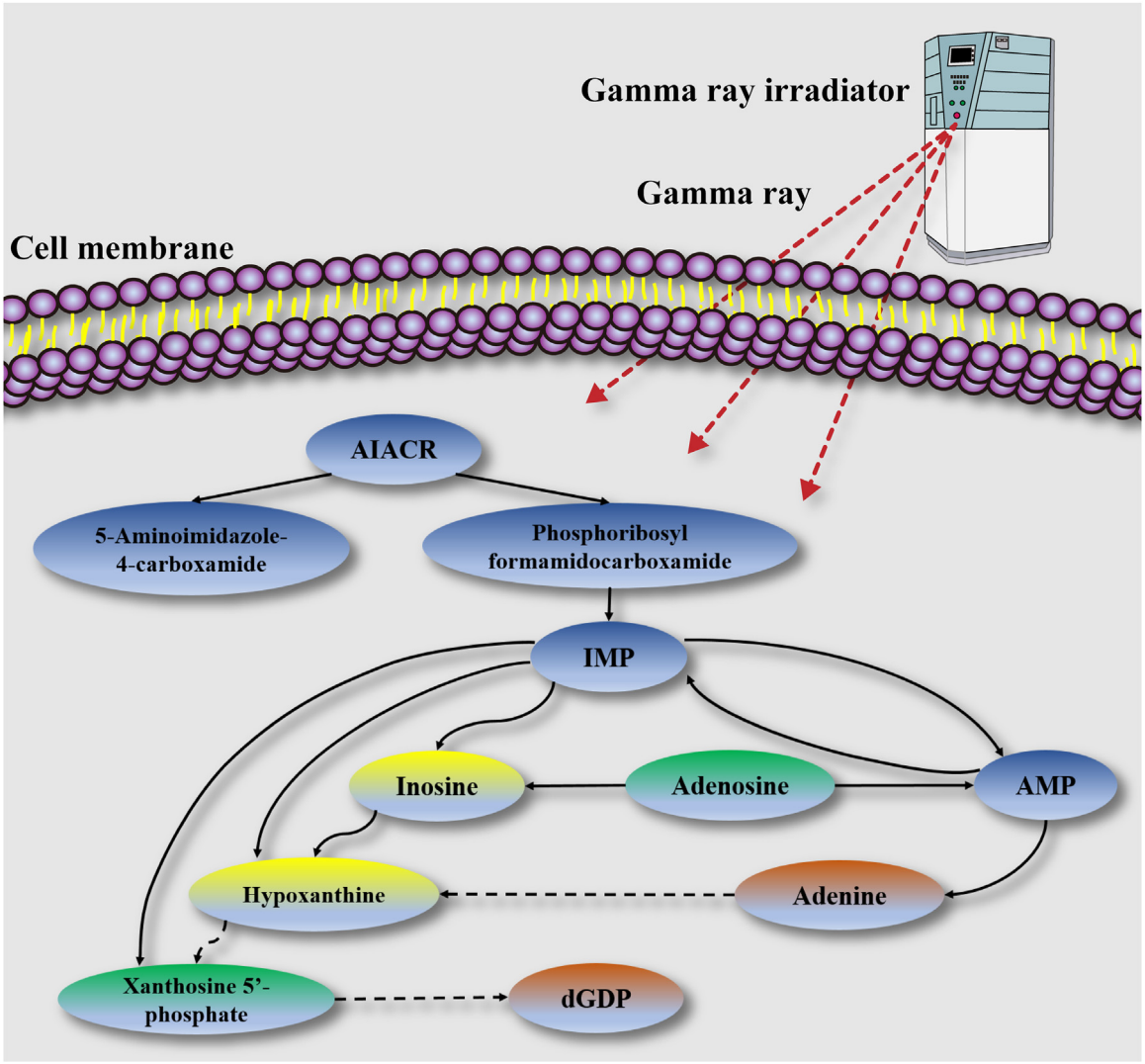

Fig. 6. Schematic of purine metabolism. Purine metabolism was affected in RBCs and PBMCs. Blue and red boxes, metabolites that were significantly decreased in RBCs and PBMCs, respectively, after irradiation. Yellow box, metabolites that decreased in RBCs but increased in PBMCs after irradiation. Green box, metabolites not detected by CIL LC–MS. Solid lines indicate direct conversion between metabolites. Dashed lines indicated that some unrelated intermediate steps have been omitted. (For interpretation of the references to colour in this figure legend, the reader is referred to the web version of this article).

Table 1
Metabolites of RBCs and PBMCs showing significant changes following irradiation.

No	Normalized RT(s)	mz_light	mz_heavy	Neutral Mass (Da)	Intensity	nCharge	nTag	Dns	HMDB	Categories
791	548.7	833.1669	837.18	366.0576	59,459	1	2		Phosphoribosyl formamidocarboxamide	
1553	947.9	815.1548	819.1696	348.0454	8614	1	2		IMP	
876	591.3	407.5904	409.597	347.0641	53614.90	2	2		AMP	RBCs
784	544.7	370.0975	372.1038	136.0392	67547.33	1	1	Hypoxanthine		
773	538.7	403.0901	405.0969	338.0635	12451.47	2	2		AICAR	
1487	918	297.0859	299.0925	126.0551	6648.4	2	2		5-Aminoimidazole-4-carboxamide	
1520	937.1	368.0992	370.1058	268.0817	11004.25	2	2		Inosine	
730	624.6	369.1131	371.119	135.0548	142960.73	1	1	Adenine		
747	632.6	370.0973	372.1034	136.039	83706.33	1	1		Hypoxanthine	PBMCs
402	447.1	661.088	663.0942	427.0297	8932.57	1	1		dGDP	
1329	936.2	368.0992	370.1058	268.0818	514049.35	2	2		Inosine	

Abbreviation: AICAR, 5-aminoimidazole-4-carboxamide-1-β-D-ribofuranoside; IMP, inosine monophosphate; AMP, adenosine monophosphate; dGDP, deoxyguanosine diphosphate; PBMCs, peripheral blood mononuclear cells; RBCs, red blood cells; RT, retention time.

damage of DNA in PBMCs. Radiation has direct and indirect effects on DNA: the direct effects are physical and chemical changes in DNA, while the indirect effects are free radical-induced oxidative damage, such as base modification, depolymerization, and chain fracture [30]. Damage to nuclear DNA leads to inhibition of lymphocyte proliferation. The immune system is sensitive to radiation, which induces lymphocyte apoptosis, disrupts cytokine synthesis, and inhibits antibody production.

Irradiation affected purine metabolism in PBMCs. Purine metabolism includes *de novo* synthesis and the salvage pathway. *De novo* purine synthesis involves phosphoribosyl pyrophosphate (PRPP) and simple substrates, such as phosphate ribose, amino acids, and CO_2. Inosinic acid is generated and transformed into AMP and guanosine monophosphate (GMP).

Cell division mandates vigorous DNA synthesis, in the mean while nucleotide reductase system activity is strong and more nucleotide compounds are produced. However, the levels of nucleotide compounds, such as guanosine diphosphate (GDP) and adenine, were decreased after irradiation (Fig. 6). The purinergic salvage pathway alone cannot provide sufficient purine analogues for lymphocyte proliferation [31]. Decreases in the levels of nucleotide analogues arrest T lymphocytes in the G phase of the cell cycle; they also suppress responses to immune signals, phagocytosis, production of lymphocyte factors, and lymphocyte maturation [32]. Irradiation interferes with purine metabolism. Adenine is a component of nucleic acids and a coenzyme involved in the synthesis of DNA and RNA; it is used therapeutically to promote the generation of white blood cells [33]. After irradiation, the adenine content decreased, accompanied by a decrease in the adenine-mediated promotion of leukocyte proliferation. Bases can be deamidated by ionizing radiation, resulting in base mismatch during transcription and replication [34]. Hypoxanthine is a product of spontaneous deamination of adenine, which is structurally similar to guanine. Adenine may be converted into hypoxanthine to pair with cytosine [35], which could explain the increased hypoxanthine content in PBMCs associated with irradiation. Therefore, after irradiation of blood, the DNA replication capacity of PBMCs is decreased, which reduces the proliferation of PBMCs and accelerates apoptosis, finally reducing the possibility of TA-GVHD.

Irradiation at a dose of 25 Gy did not markedly affect the activity or function of RBCs. There were no significant changes in pH or hemoglobin content between the irradiated and control groups during storage [36]. However, with increasing storage time, irradiation could aggravate the storage lesions of RBCs [37]. Irradiation exacerbates some elements of RBC storage lesions. For example, irradiation promotes hemolysis of RBCs and increases the potassium ion content of plasma [10]. Recent untargeted metabolic research showed that irradiation altered arachidonic acid metabolism in RBCs [38]. Dysfunction of 8-isoprostane, a differential metabolite in this pathway, may cause the RBC membrane to harden and lose its ability to deform. As shown in Fig. 6, AMP production in RBCs was decreased by irradiation. AMP, which consists of the nucleobase adenine, the sugar ribose, and a phosphate group, is converted into adenosine diphosphate and then into ATP, which is a signaling molecule in purine metabolism that mediates energy exchange [39]. Our results showed that the effects of irradiation on erythrocyte ATP level were not clinically significant [40]. The ratio of AMP to ATP presumably decreases after irradiation. An increase in AMP/ATP content enhances cellular repair ability [41]. Taken together, the results indicated that, although irradiation has minimal effect on RBCs, it may influence their preservation in storage due to the decrease in AMP content.

Taurine and hypotaurine metabolism in plasma was affected by irradiation. Irradiation significantly increased the hypotaurine content in both males and females. Irradiation damages the RBC membranes and reduces antioxidant activity in these cells [42]. Hypotaurine acts as an antioxidant by scavenging hydroxyl radicals [43] to repair irradiation-induced damage. Hypotaurine is also the precursor of taurine [44], and both are concentrated in leukocytes. Taurine increases the number of leukocytes [45] and its metabolism is modulated by stress [46]. Hypotaurine may show a compensatory increase when the proliferation of PBMCs is inhibited by irradiation.

This study had several limitations. We did not examine the dynamic changes in metabolism in irradiated blood during storage. Moreover, further studies with larger sample sizes are required to verify the results. There were no significant differences in the levels of potassium and ATP before and after irradiation, indicating that the quality of blood was not significantly altered by irradiation. The total number of RBCs and hemoglobin level were not significantly altered after irradiation. White blood cells and lymphocytes, as well as the proportions of lymphocytes and monocytes, were decreased by irradiation; however, they remained within the respective normal ranges. The apoptosis of PBMCs was increased and their proliferation was inhibited. Changes in the contents of adenine and hypoxanthine as components of purine metabolism in PBMCs may have inhibited DNA synthesis and thus inhibited the proliferation of these cells. These results indicated that irradiation prevented TA-GVHD, but had minimal effects on plasma and RBCs. Increased levels of hypotaurine in plasma may repair radiation damage. However, the decrease in AMP level in RBCs suggests that irradiation would influence the quality of these cells during storage, and therefore the addition of AMP should be considered to preserve RBCs during storage. We suggest that irradiation of blood should be promoted in clinical practice, and that it should be transfused earlier after irradiation.

5. Conclusions

In conclusion, a $^{12}C/^{13}C$-dansylation labeling LC–MS metabolic detecting technique was used to investigate the effects of irradiation on metabolism in blood components. Irradiation had marked effects on the metabolism of blood components, particularly lymphocyte proliferation and apoptosis, as well as the preservation of RBCs. Taurine and hypotaurine metabolism in plasma and purine metabolism in PBMCs and RBCs were affected by irradiation. The significant metabolites were adenine and hypoxanthine in PBMCs, AMP in RBCs, and hypotaurine in plasma. Our research provided a comprehensive overview of metabolic changes after blood irradiation, and provided a basis for further studies to optimize the use of irradiated blood in clinical settings.

CRediT authorship contribution statement

Hongcui Cao and **Senxiang Yan**: conception and design; **Xuan Lu** and **Xinli Zhu**: assisted to design the study and prepared the cells. **Deying Chen** and **Jiahang Zhou**: technical support; **Xuan Lu**, **Jiahang Zhou** and **Jiong Yu**: analyzed the data; **Xuan Lu** and **Xinli Zhu**: drafted the manuscript. **Liang Li**: Supervised the study; **Lanjuan Li**: Project administration.

Declaration of Competing Interest

The authors report no declarations of interest.

Acknowledgments

This work was supported by grants for Stem Cell and Translational Research from National Key Research and Development Program of China (No. 2020YFA0113003).

Appendix A. Supplementary data

Supplementary material related to this article can be found, in the online version, at doi:https://doi.org/10.1016/j.jpba.2021.114247.

References

[1] G.C. Leitner, et al., Altered intracellular purine nucleotides in gamma-irradiated red blood cell concentrates, Vox Sang. 81 (2001) 113–118.

[2] J. Treleaven, et al., Guidelines on the use of irradiated blood components prepared by the British Committee for Standards in Haematology blood transfusion task force, Br. J. Haematol. 152 (1) (2011) 35–51.
[3] P. Manduzio, Transfusion-associated graft-versus-host disease: a concise review, Hematol. Rep. 10 (4) (2018) 7724.
[4] H. Ruhl, G. Bein, U.J. Sachs, Transfusion-associated graft-versus-host disease, Transfus. Med. Rev. 23 (1) (2009) 62–71.
[5] K.J. Gelly, R.K, S. Rawlinson, A. Norris, D. T, Transfusion-associated graft vs. host disease in a patient withhigh-grade B-cell lymphoma. Should cellular products forpatients with non-Hodgkin's lymphoma be irradiated, Br. J. Haematol. 110 (1) (2000) 228–229.
[6] A.G. Rolink, G.E, Allosuppressor- and allohelper-T cells in acute and chronic graft-vs.-host (GVH) disease. III. Different lyt subsets of donor t cells induce different pathological syndromes, J. Exp. Med. 158 (2) (1983) 546–558.
[7] P. Sen, et al., Metabolic alterations in immune cells associate with progression to type 1 diabetes, Diabetologia 63 (5) (2020) 1017–1031.
[8] L.D. Fast, Developments in the prevention of transfusion-associated graft-versus-host disease, Br. J. Haematol. 158 (5) (2012) 563–568.
[9] J.L. Carson, et al., Clinical practice guidelines from the AABB: red blood cell transfusion thresholds and storage, JAMA 316 (19) (2016) 2025–2035.
[10] D. de Korte, et al., Timing of gamma irradiation and blood donor sex influences in vitro characteristics of red blood cells, Transfusion 58 (4) (2018) 917–926.
[11] T. Nemkov, et al., Metabolomics in transfusion medicine, Transfusion 56 (4) (2016) 980–993.
[12] A. Sreekumar, et al., Metabolomic profiles delineate potential role for sarcosine in prostate cancer progression, Nature 457 (7231) (2009) 910–914.
[13] Z.H. Yang, et al., Metabolic profiling reveals biochemical pathways and potential biomarkers of spinocerebellar ataxia 3, Front. Mol. Neurosci. 12 (2019) 159.
[14] B. Zhou, et al., LC-MS-based metabolomics, Mol. Biosyst. 8 (2) (2012) 470–481.
[15] B. Chutvirasakul, et al., Development and applications of liquid chromatography-mass spectrometry for simultaneous analysis of anti-malarial drugs in pharmaceutical formulations, J. Pharm. Biomed. Anal. 195 (2021) 113855.
[16] D. Chen, et al., Overcoming sample matrix effect in quantitative blood metabolomics using chemical isotope labeling liquid chromatography mass spectrometry, Anal. Chem. 89 (17) (2017) 9424–9431.
[17] D. Chen, et al., Chemical isotope labeling LC–MS for monitoring disease progression and treatment in animal models: plasma metabolomics study of osteoarthritis rat model, Sci. Rep. 7 (2017) 40543.
[18] T. Huan, L. Li, Quantitative metabolome analysis based on chromatographic peak reconstruction in chemical isotope labeling liquid chromatography mass spectrometry, Anal. Chem. 87 (14) (2015) 7011–7016.
[19] K. Guo, L. Li, High-performance isotope labeling for profiling carboxylic acid-containing metabolites in biofluids by mass spectrometry, Anal. Chem. 82 (21) (2010) 8789–8793.
[20] K. Guo, L. Li, Differential 12C-/13C-isotope dansylation labeling and fast liquid chromatography/mass spectrometry for absolute and relative quantification of the metabolome, Anal. Chem. 81 (10) (2009) 3919–3932.
[21] P. Bruheim, H.F. Kvitvang, S.G. Villas-Boas, Stable isotope coded derivatizing reagents as internal standards in metabolite profiling, J. Chromatogr. A 1296 (2013) 196–203.
[22] C. Bueschl, et al., Isotopic labeling-assisted metabolomics using LC-MS, Anal. Bioanal. Chem. 405 (1) (2013) 27–33.
[23] S. Gehrke, et al., Metabolomics evaluation of early-storage red blood cell rejuvenation at 4°C and 37°C, Transfusion 58 (8) (2018) 1980–1991.
[24] X. Shi, et al., MSC-triggered metabolomic alterations in liver-resident immune cells isolated from CCl4-induced mouse ALI model, Exp. Cell Res. 383 (2) (2019) 111511.
[25] J. Jiao, et al., Comparison of two commonly used methods for stimulating T cells, Biotechnol. Lett. 41 (12) (2019) 1361–1371.
[26] R. Zhou, et al., IsoMS: automated processing of LC-MS data generated by a chemical isotope labeling metabolomics platform, Anal. Chem. 86 (10) (2014) 4675–4679.
[27] T. Huan, L. Li, Counting missing values in a metabolite-intensity data set for measuring the analytical performance of a metabolomics platform, Anal. Chem. 87 (2) (2015) 1306–1313.
[28] T. Huan, et al., DnsID in MyCompoundID for rapid identification of dansylated amine- and phenol-containing metabolites in LC-MS-based metabolomics, Anal. Chem. 87 (19) (2015) 9838–9845.
[29] J.X. Mi, et al., Principal component analysis based on nuclear norm minimization, Neural Netw. 118 (2019) 1–16.
[30] K. Suzuki, et al., Radiation-induced DNA damage and delayed induced genomic instability, Oncogene 22 (45) (2003) 6988–6993.
[31] Y.M. Marijnen, et al., Studies on the incorporation of precursors into purine and pyrimidine nucleotides via' de novo' and' salvage' pathways in normal lymphocytes and lymphoblastic cell-line cells, Biochim. Biophys. Acta 1012 (2) (1989) 148–155.
[32] A.D. Kulkarni, F.B. Rudolph, C.T. Van Buren, The role of dietary sources of nucleotides in immune function: a review, J. Nutr. 124 (Suppl. 8) (1994) 1442s–1446s.
[33] M.M. Müller, et al., Adenine and hypoxanthine metabolism in phythohemagglutinin-stimulated and unstimulated human lymphocytes, Blut 40 (2) (1980) 137–145.
[34] L.M. Martin, et al., DNA mismatch repair and the DNA damage response to ionizing radiation: making sense of apparently conflicting data, Cancer Treat. Rev. 36 (7) (2010) 518–527.
[35] W.P. Roos, B. Kaina, DNA damage-induced cell death: from specific DNA lesions to the DNA damage response and apoptosis, Cancer Lett. 332 (2) (2013) 237–248.
[36] F. Adams, et al., Metabolic effects occurring in irradiated and non-irradiated red blood cellular components for clinical transfusion practice: an in vitro comparison, Afr. J. Lab. Med. 7 (1) (2018) 606.
[37] A.C. Zubair, Clinical impact of blood storage lesions, Am. J. Hematol. 85 (2) (2010) 117–122.
[38] R.M. Patel, et al., Metabolomics profile comparisons of irradiated and nonirradiated stored donor red blood cells, Transfusion 55 (3) (2015) 544–552.
[39] M. Bonora, et al., ATP synthesis and storage, Purinergic Signal. 8 (3) (2012) 343–357.
[40] R. Zimmermann, et al., Influence of late irradiation on the in vitro RBC storage variables of leucoreduced RBCs in SAGM additive solution, Vox Sang. 100 (3) (2011) 279–284.
[41] M.A. Menze, M.J. Clavenna, S.C. Hand, Depression of cell metabolism and proliferation by membrane-permeable and -impermeable modulators: role for AMP-to-ATP ratio, Am. J. Physiol. Regul. Integr. Comp. Physiol. 288 (2) (2005) R501–10.
[42] M.A. Acosta-Elias, et al., Nano alterations of membrane structure on both gamma-irradiated and stored human erythrocytes, Int. J. Radiat. Biol. 93 (12) (2017) 1306–1311.
[43] O.I. Aruoma, et al., The antioxidant action of taurine, hypotaurine and their metabolic precursors, Biochem. J. 256 (1) (1988) 251–255.
[44] N. Masuoka, et al., High-performance liquid chromatographic determination of taurine and hypotaurine using 3,5-dinitrobenzoyl chloride as derivatizing reagent, J. Chromatogr. B (1994) 31–35.
[45] L. Wang, et al., Effect of taurine on leucocyte function, Eur. J. Pharmacol. 616 (1–3) (2009) 275–280.
[46] F. Fazzino, F. Obregón, L. Lima, Taurine and proliferation of lymphocytes in physically restrained rats, J. Biomed. Sci. 17 (Suppl. 1) (2010) S24.